Fusion Engineering and Design 100 (2015) 571–575

Contents lists available at ScienceDirect

Fusion Engineering and Design

journal homepage: www.elsevier.com/locate/fusengdes

Effect of mechanical milling on the microstructure of tungsten under He^+ irradiation condition

Xiao-Yue Tan[a], Ping Li[a,c], Lai-Ma Luo[a,c,*], Hong-Yu Chen[a], Xiang Zan[a,c], Xiao-Yong Zhu[a,c], Guang-Nan Luo[b], Yu-Cheng Wu[a,c,*]

[a] School of Materials Science and Engineering, Hefei University of Technology, Hefei 230009, China
[b] Institute of Plasma Physics, Chinese Academy of Sciences, Hefei 230031, China
[c] National–Local Joint Engineering Research Centre of Nonferrous Metals and Processing Technology, Hefei 230009, China

ARTICLE INFO

Article history:
Received 5 April 2015
Received in revised form 7 July 2015
Accepted 17 August 2015
Available online 29 August 2015

Keywords:
Plasma facing material
Tungsten
Helium irradiation
Spark plasma sintering

ABSTRACT

"Pure" W was prepared through a powder metallurgy route by using hard alloy (WC–Co) milling tank and balls to mill WO_3 powder, reducing with high purity H_2, and sintering with spark plasma sintering technique. XRD, SEM, and TEM were used to characterize the phase and phase structures. Results showed that the cobalt tungsten carbide ($Co_3W_{10}C_{3.4}$) phase was induced from the milling tank and balls. After the "pure" W bulk was exposed to helium ions for 2 h, the cobalt tungsten carbide phase was found to be surrounded by the lattice distortion phase of W, which showed high irradiation resistance.

1. Introduction

Tungsten and its alloys, which exhibit excellent performance with their high melting point, high thermal conductivity, high strength at elevated temperatures, low sputtering yield under radiation environment, and low tritium inventory, have been regarded as the most promising plasma facing materials for future fusion reactors [1–3]. Nanostructured W-matrix materials were proposed to improve irradiation resistance by providing sufficient grain boundaries to act as point of annihilation for radiation-induced defects [4–7]. Preparation of nanosized powders is an effective approach to improve sintering activity and could yield fine-grained W-matrix materials [8,9]. Traditional mechanical milling is a successful method of preparing nanosized powders for mass production [10–12].

During mechanical milling, formation of a second phase, which is introduced from the wear of milling equipment and media, can significantly affect microstructural development and material properties [13]. These second phase result in increased hardness and weakened thermal conductivity. However, the microstructure evolution of W induces this second-phase material under fusion circumstances, which is worth studying. In this paper, hard alloy milling tank and balls, which are composed of 96% WC and 4% Co, were used. Compare to the traditional stainless steel tank and balls, the hard alloy possess of high melting point and high hardness, which would have a significant milling effect and result induced impurities as less as possible, especially low-melting impurities. Milling with WO_3 powder, reduction by high-purity H_2, and then sintering by spark plasma sintering (SPS) technique were performed. The obtained sample was exposed to a high-flux, high-fluence, lower-energy, and long-duration helium plasma, which could result in serious microstructure damage.

2. Experimental

2.1. Preparation of materials

WO_3 (>99.0% purity, AR, Sinopharm Chemical Reagent Co., Ltd, Shanghai, China) was used as the raw material. To obtain micro-sized powder particles, WO_3 was loaded in a planetary mill (XGB2, Nanjing University Instrument plant, Nanjing, China) with hard alloy balls in a hard ally milling tank at a speed of 400 rpm. The powder was wet-milled with an ethanol solution at a ball-to-powder weight ratio of 15:1. After wet-milling for 36 h, the powder was dried at 60 °C and then ground in an agate mortar. The obtained dried powders were reduced by highly pure H_2 in a tubular furnace.

* Corresponding authors at: School of Materials Science and Engineering, Hefei University of Technology, Hefei 230009, China. Tel.: +86 551 62901012; fax: +86 551 62901012.
E-mail addresses: luolaima@126.com (L.-M. Luo), ycwu@hfut.edu.cn (Y.-C. Wu).

http://dx.doi.org/10.1016/j.fusengdes.2015.08.006
0920-3796/

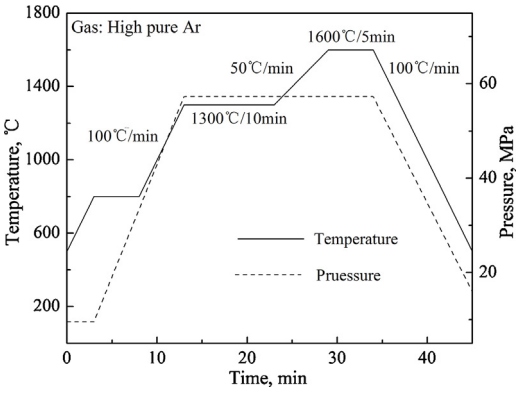

Fig. 1. Sintering curve for the reduction powder.

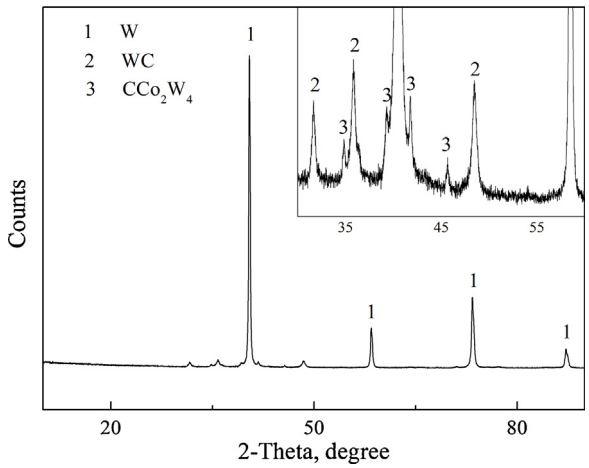

Fig. 2. XRD pattern of the reduced WO_3 powder; the inset image was the amplification of the pattern in 2-Theta between 30 to 60 degree.

In the reduction process, the temperature was raised at a heating rate of 5 °C/min to 500 °C and held for 1 h, and then to 850 °C and held for 90 min. Then, the samples were cooled down to room temperature at a cooling rate of 5 °C/min under hydrogen flow.

The reduced powder was sintered by spark plasma sintering (SPS, FCT Group, SE-607, Germany). The powder was loaded in an electrically and thermally conductive graphite die with a diameter of approximately 20 mm. Then, a DC current is applied in pulses and was assisted by a high uniaxial mechanical pressure during the process. The sintering curve is shown in Fig. 1. At first, the sample was heated to 500 °C, and the pressure load was 9.6 MPa. The sample was then heated to 800 °C at a rate of 100 °C/min and dwelled for 5 min to relieve the residual gas in this powder. During the process, the pressure was retained at 9.6 MPa for 4 min and was uniformly increased to 57.3 MPa in 10 min. This pressure was then kept constant for the duration of the following sintering processes. Simultaneously, the sample was heated to 1300 °C at a heating rate of 100 °C/min. At the following stage, the sample was kept at 1300 °C for 10 min and subsequently heated to 1600 °C at a heating rate of 50 °C/min. The sample was sintered at 1600 °C for 3 min and then cooled down to room temperature at a cooling rate of about 100 °C/min. At the same time, the pressure was uniformly decreased. This sintering process was carried out in a protective of Ar atmosphere to prevent sample oxidation.

Mirror-quality polished W plates were implanted with He^+ ion beams for 2 h and maintained at room temperature using Large-Power Materials Irradiation Experiment System (LP-MIES). During He^+ irradiation, the temperature of the targets was measured via infrared thermometer. The corresponding beam energy was 80 eV, and the He^+ ion beam flux remained constant at 1.2×10^{22} ions/(m^2 s), resulting in a surface temperature of 1100 °C. The He^+ ion fluence was approximately 8.64×10^{25} ions/m^2 during implantation experiments.

2.2. Characterization

X-ray diffraction (XRD) patterns were used to characterize the reduced powders and the sintered sample. The powder, surface, and fracture morphology of the sample were examined using the field-emission scanning electron microscopy (FE-SEM, SU8020, Japan) equipped with energy-dispersive spectrometer (EDS). The true density of the sintered body was measured by Archimedes principle. A layer on the back surface, which presents a loose structure, could be viewed by naked-eye inspection after irradiation. The microstructure of the irradiation region was observed by transmission electron microscopy (TEM, JEM-2100F, Japan). To prepare the TEM specimen, the surface of the irradiation-damaged region was scraped by a knife, placed in ethanol solution, and dispersed by ultrasonic wave. The above-prepared solution was titrated on a copper mesh with a drip pipe and used for TEM analysis.

3. Results and discussion

3.1. Characterization of powders

The XRD pattern of the reduced powders is presented in Fig. 2, which shows that the reduced powder consisted of W main phase of W (JCPDS no. 89-2767), as well as small amounts of WC (JCPDS no. 89-2727) and CCo_2W_4 (JCPDS no. 06-0611), which are the basis of the weak peaks shown in the inset image in Fig. 2. W should result from the reduction of tungsten oxide (WO_3), and WC and cobalt tungsten carbide must derive from the hard alloy milling tank and balls, which are composed of WC and Co. According to the peaks in the XRD pattern, the powder underwent an alloying process after H_2 reduction.

The FE-SEM morphology of ball-milled WO_3 and reduced W powders are presented in Fig. 3. As shown in Fig. 3a, the average particle size of the ball-milled WO_3 powders are range from 200 nm to 400 nm, and exhibit a certain degree of aggregation. Large-sized particles resulted from the aggregation of smaller-sized particles. In Fig. 3b, the reduced W powders with an average particle size of 200 nm to 600 nm, and present no apparent aggregation. For the aggregation milled powder, in particular, the reduced powder particles grew during the reduction process. From Fig. 3b, distinguishing the W, WC and CCo_2W_4 phases, which can be detected in the XRD pattern, is difficult.

3.2. Characterization of the sintered body

After the reduced powder was sintered by SPS, XRD was used to characterize the phase of the materials, as shown in Fig. 4. The main peaks of the pattern was demarcated with the W phase, and the weak peaks indicate the second phase of cobalt tungsten carbide ($Co_3W_{10}C_{3.4}$, JCPDS no. 71-0173), which is marked in the inset of Fig. 4. Compared with the reduced-powder XRD pattern (Fig. 2), no peaks of WC and CCo_2W_4 were found, meaning that the formation of $Co_3W_{10}C_{3.4}$ should result from WC and CCo_2W_4 during the sintering process. Impurity elements Co and C are induced from the milling tank and balls (composed of WC and Co), which solvate with W and form the solid $Co_3W_{10}C_{3.4}$ solution.

The XRD spectrum of the sintered body was also used to quantitative analysis the content of the impurity phase of $Co_3W_{10}C_{3.4}$, and result shows that the content of $Co_3W_{10}C_{3.4}$ was about 8.6 wt.%. The